

Quantum phase transitions in CePdAl probed by ultrasonic and thermoelectric measurements

Hengcan Zhao(赵恒灿), Meng Lyu(吕孟), Jiahao Zhang(张佳浩), Shuai Zhang(张帅), and Peijie Sun(孙培杰)
Citation: Chin. Phys. B, 2022, 31 (**11**): 117103. DOI: 10.1088/1674-1056/ac8345

What follows is a list of articles you may be interested in

Investigation of electronic, elastic, and optical properties of topological electride Ca_3Pb via first-principles calculations

Chang Sun(孙畅), Xin-Yu Cao(曹新宇), Xi-Hui Wang(王西惠), Xiao-Le Qiu(邱潇乐), Zheng-Hui Fang(方铮辉), Yu-Jie Yuan(袁宇杰), Kai Liu(刘凯), and Xiao Zhang(张晓)
Chin. Phys. B, 2021, 30 (**5**): 057104. DOI: 10.1088/1674-1056/abec38

Structure prediction, electronic, and mechanical properties of alkali metal MB_{12} (*M*= *Be*, Mg, Ca, Sr) from first principles

Chun-Ying Pu(濮春英), Rong-Mei Yu(于荣梅), Ting Wang(王婷), Zhen-Yan X\"ue(薛振彦), Yong-Sheng Zhu(朱永胜), and Da-Wei Zhou(周大伟)
Chin. Phys. B, 2021, 30 (**1**): 017102. DOI: 10.1088/1674-1056/abb667

Ab initio study of structural, electronic, thermo-elastic and optical properties of Pt_3Zr intermetallic compound

Wahiba Metiri, Khaled Cheikh
Chin. Phys. B, 2020, 29 (**4**): 047101. DOI: 10.1088/1674-1056/ab7223

Heavy fermions in high magnetic fields

M Smidman, B Shen(沈斌), C Y Guo(郭春煜), L Jiao(焦琳), X Lu(路欣), H Q Yuan(袁辉球)
Chin. Phys. B, 2019, 28 (**1**): 017106. DOI: 10.1088/1674-1056/28/1/017106

Voltage-controlled Kosterlitz-Thouless transitions and various kinds of Kondo behaviors in a triple dot device

Yong-Chen Xiong(熊永臣), Jun Zhang(张俊), Wang-Huai Zhou(周望怀), Amel Laref
Chin. Phys. B, 2017, 26 (**9**): 097102. DOI: 10.1088/1674-1056/26/9/097102

Quantum phase transitions in CePdAl probed by ultrasonic and thermoelectric measurements

Hengcan Zhao(赵恒灿)[1], Meng Lyu(吕孟)[1], Jiahao Zhang(张佳浩)[1], Shuai Zhang(张帅)[1], and Peijie Sun(孙培杰)[1,2,3,†]

[1] *Beijing National Laboratory for Condensed Matter Physics, Institute of Physics, Chinese Academy of Sciences, Beijing* 100190, *China*
[2] *School of Physical Science, University of Chinese Academy of Sciences, Beijing* 100049, *China*
[3] *Songshan Lake Materials Laboratory, Dongguan* 523808, *China*

(Received 24 June 2022; revised manuscript received 20 July 2022; accepted manuscript online 22 July 2022)

CePdAl has been recently recognized as a frustrated antiferromagnetic heavy-fermion compound with a pressure- or field-tuned, extended quantum critical phase at zero temperature. Identifying characteristic signatures of the emerging quantum critical phase, which are expected to be distinct from those near a quantum critical point, remains challenging. In this work, by performing ultrasonic and thermoelectric measurements down to very low temperatures in a ^{3}He–^{4}He dilution refrigerator in the presence of magnetic field, we are able to obtain some crucial thermodynamic and thermal transport features of the quantum critical phase, including a frustration-related elastic softening detected by ultrasound and a Fermi-surface change probed by thermoelectric effect.

Keywords: quantum phase transition, ultrasound, elastic constant, thermoelectric power

PACS: 71.27.+a, 73.43.Nq, 75.30.Mb **DOI:** 10.1088/1674-1056/ac8345

1. introduction

Quantum phase transitions (QPTs) are those that are driven by quantum instead of thermal fluctuations at low enough temperatures.[1,2] They are at the forefront of current condensed matter physics, offering possibilities for a variety of quantum emergent phenomena in their vicinity including unconventional superconductivity and non-Fermi liquid.[3,4] Heavy-fermion materials are ideal systems for exploring QPTs due to the competition between the intersite Ruderman–Kittel–Kasuya–Yoshida (RKKY) interaction and the local Kondo effect. Prototypical examples are second-order antiferromagnetic (AFM) QPTs which can be smoothly suppressed to absolute zero at a quantum critical point (QCP) by nonthermal tuning parameters like magnetic field and pressure, beyond which a heavy Fermi-liquid phase develops generically as depicted by the Doniach phase diagram.[5]

Thus far, various low-temperature probes have been employed to detect potential QPTs in heavy-fermion materials. Among these, electrical resistivity provides probably the simplest approach through its temperature dependence that frequently deviates from the Fermi-liquid description. On the other hand, low-temperature Hall effect has emerged as a powerful measurement to identify the characteristic feature of Mott-type QPTs, where breakdown of the local Kondo effect occurs with a consequent change of Fermi-surface volume.[6] In addition, thermodynamic and magnetic responses such as the coefficients of electronic specific heat and thermal expansion, and the magnetic susceptibility usually show diverging behavior near a QCP.[2,4] These probes are nevertheless frequently insufficient in characterizing complicated QPTs in, for example, a geometrically frustrated Kondo lattice with enhanced quantum fluctuations and potential metallic spin-liquid phase.[7]

Hexagonal CePdAl shows rich quantum states due to magnetic frustration associated with the distorted kagome lattice.[7,8] At ambient pressure and zero field, it undergoes an AFM transition at $T_{\rm N} = 2.7$ K with only 2/3 of the Ce moments on the kagome lattice involved,[9] see Fig. 1(a) inset. The other 1/3 is Kondo screened, giving rise to the heavy-fermion behavior with an electronic specific-heat coefficient $\gamma = 270$ mJ/mol·K^2 (Ref. [10]). Applying magnetic field along the Ising moment (the c axis) causes three AFM phases (a–c) in the low-field phase space that are terminated by three first-order metamagnetic lines (B_{ab}, B_{bc}, and B_{cp}), see Fig. 1(a). Further increasing field leads to a quantum critical phase (p) before a Fermi-liquid phase (f) eventually settles down. Alternatively, the AFM phase can be smoothly suppressed to zero by hydrostatic pressure as well, with no metamagnetic transitions taking place. In this case, a much more extended p phase can be identified by the linear-in-temperature resistivity, a hallmark of non-Fermi-liquid behavior.[7] At elevated temperatures $T > 1$ K, except for the $T_{\rm N}(B)$ line which traces the smoothly reduced AFM transition, two additional lines $B_m(T)$ and $B^*(T)$ are also shown in Fig. 1(a). B_m is related to the onset of AFM short-range order and B^* indicates the Mott-type Fermi-surface crossover, which terminates at a Kondo-breakdown QCP at zero temperature. As shown in Fig. 1(b), the three metamagnetic transitions can be simply identified by

†Corresponding author. E-mail: pjsun@iphy.ac.cn

© 2022 Chinese Physical Society and IOP Publishing Ltd

resistivity as a function of field, revealed as sharp anomalies in $\mathrm{d}\rho/\mathrm{d}B$, where the existence of the p phase can be confirmed by a shallow shoulder.

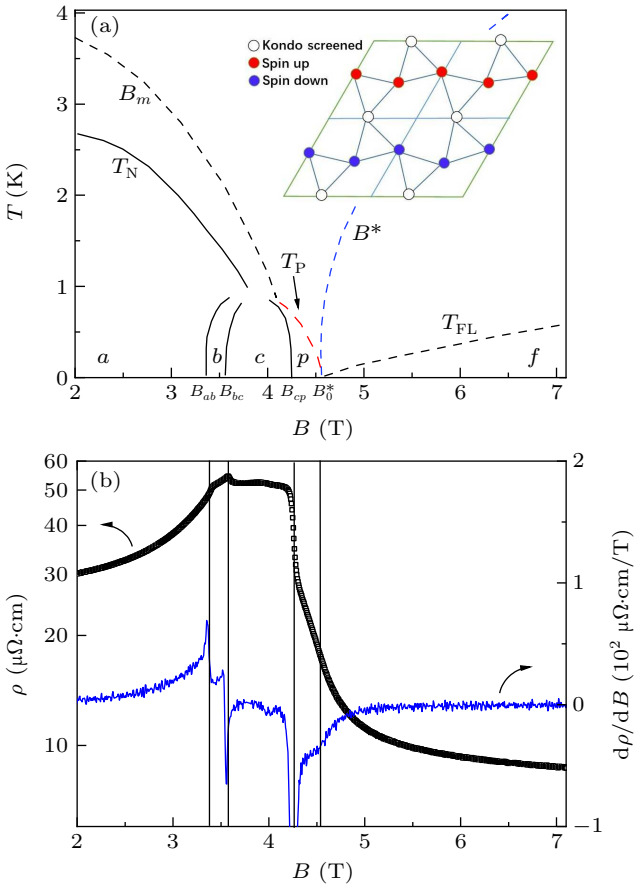


Fig. 1. (a) Field–temperature phase diagram of CePdAl adapted from Ref. [8]. See text for definition of the symbols used in this figure. Inset illustrates the in-plane magnetic structure determined by neutron powder diffraction.[9] (b) Isothermal resistivity ρ and the derivative $\mathrm{d}\rho/\mathrm{d}B$ as a function of field measured at 0.08 K, from which all the low-temperature phase boundaries can be identified (see vertical lines). Different to the sharp anomalies at the three metamagnetic transitions, the Mott-type transition at $B^* \approx 4.6$ T behaves as a shallow shoulder in $\mathrm{d}\rho/\mathrm{d}B$.

This work aims to demonstrate some distinctive features of the quantum critical phase and the related Fermi-surface change in CePdAl by low-temperature ultrasonic and thermoelectric measurement, both of which have so far received much less attention in studying QPTs. Ultrasound can probe magnetic, electronic and lattice instability sensitively because of the spin-lattice and electron–phonon coupling. Heavy-fermion materials are particularly suited for such measurement due to their strongly volume-dependent hybridization effect between the localized f electrons and the conduction bands that is described by a strong electron–phonon coupling.[11,12] Likewise, thermoelectric effect measures particle–hole asymmetric band structure at the Fermi level and is therefore suited for detecting Mott-type QPTs where a Fermi-surface change takes place. As will be shown below, the two measurements have revealed characteristic and unique features in support of the occurrence of a frustration-assisted intermediate quantum critical phase and a Fermi-surface change in CePdAl.

2. Experimental details

The ultrasound measurements were performed by using phase comparison technique[13] — a well-established method for probing weak elastic change of solid materials by comparing the input and output ultrasound pulse. High-frequency ultrasound of typically 5 MHz–100 MHz is generated and detected by $LiNiO_3$ piezoelectric transducers that are bonded onto two parallel end faces of the sample to be studied, see the inset of Fig. 2. Thiokol liquid polymer is used as bond material between the transducers and the sample. The relative ultrasound velocity change $\delta\upsilon/\upsilon$ during a temperature or field scan is proportional to the sum of three parts: the frequency change $\delta f/f$ and the phase shift $\delta\psi/\psi$ of the input and output ultrasound waves, and the sample length change $\delta L/L$, which is however negligible in most cases compared to the former two terms. In this technique the frequency of the input ultrasound wave is continuously adjusted in order to maintain a constant phase of a given output echo ($\delta\psi = 0$), one can therefore probe $\delta\upsilon/\upsilon$ simply by monitoring $\delta f/f$. Elastic constant C can be calculated from the sound velocity, $C = d\upsilon^2$, with d being the sample density. To ensure a sufficient thermal conductance for achieving temperatures down to below 50 mK, the transducers were bonded on one side by silver paste to the cooper plate that is thermally coupled to the cold finger of a ^{3}He–^{4}He dilution refrigerator. The typical sample thickness for ultrasound measurement is 1 mm–3 mm and a single crystal has to be used in order to probe multiple independent elastic modes of the elastic constant tensor.[13]

The thermoelectric effect was measured with a standard setting of thermal-transport measurement by using two thermometers and one heater. A sample of a typical size 0.3 mm × 0.5 mm × 3.0 mm was used and mounted onto a silver block by silver paste that is directly screwed to the sample holder.[14] The thermometers and heater are, on one hand, suspended by fine nylon wires in a vespel frame in order to be thermally decoupled from their surroundings, and on the other hand, thermally coupled to the sample by using 50-μm gold wires in order to build and measure the temperature gradient δT, which is typically 2%–5% of the base temperature. We use RuO_2 bare resistive chip sensor (Lake Shore Cryotronics) as thermometer, and 1-kΩ chip resistor as heater. For electrical leads in the sample holder superconducting NbTi wires ($\phi = 25$ μm) were used. The measurement was performed in a dilution refrigerator down to approximately 50 mK.

3. Results and discussion

Figure 2 shows relative change of the elastic constants C_{11} and C_{33} measured at 80 mK in the presence of a sweeping magnetic field ($B\|c$). They both are longitudinal elastic mode, measured with the ultrasound wave propagating/polarizing

along the a and c axis (Fig. 2 inset), respectively. Upon increasing field, the two elastic constants soften smoothly due to enhanced spin fluctuations, and the first-order metamagnetic transitions at B_{ab} and B_{bc} manifest themselves as a drastic drop. The field variation of elasticity is similar for $\delta C_{11}/C_{11}(B)$ and $\delta C_{33}/C_{33}(B)$ up to slightly below $B_{cp} \approx 4.2$ T, conforming to the low-temperature coefficient of magnetostriction, where sharp peaks indicative of significant lattice-parameter change are observed at the metamagnetic transitions.[15] Further increase of magnetic field results in the most fascinating p phase in this material, where $\delta C_{11}/C_{11}(B)$ and $\delta C_{33}/C_{33}(B)$ behave totally differently: at the phase boundary between the magnetic phase c and the quantum critical p phase, B_{cp}, the former elastic mode reveals a strong softening, whereas the latter turns harder drastically. Consequently, a significant elastic softening is observed in only $C_{11}(B)$ in the emerging quantum critical p phase, see the shaded region in Fig. 2. This distinctive feature offers a piece of compelling evidence for the existence of the p phase. Furthermore, the contrasting elastic behavior between the two elastic modes within the quantum critical phase provides a straightforward and strong implication on the microscopic origin of this phase. Considering that C_{11} measures the response of the compressional ultrasound wave within the ab plane that is composed of distorted kagome lattice, whereas C_{33} measures along the c axis, one can naturally infer that the additional elastic softening in the p phase observed solely in C_{11} is caused by the in-plane magnetic frustration. On the other hand, the smooth hardening in the heavy Fermi-liquid regime reflects, at least partially, the increased energy scale of the Fermi-liquid phase ($T_{\rm FL}(B)$, Fig. 1(a)) and the therefore modified electron–phonon coupling.[12]

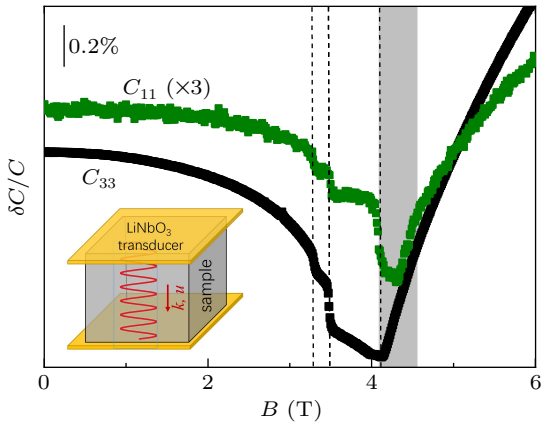


Fig. 2. Relative changes of the isothermal elastic constants C_{11} and C_{33} measured by longitudinal ultrasound propagating along the a and c axes, respectively, as a function of field ($B\|c$) at $T = 80$ mK. Note that $\delta C_{11}/C_{11}$ is multiplied by a factor of 3 for better comparison. The three dashed lines indicate the positions of the metamagnetic critical fields B_{ab}, B_{bc}, and B_{cp}. The shaded region marks the field window where the quantum critical p phase takes place, see Fig. 1(a). Inset: a sketch of the sample setting for ultrasound measurement, where the directions of propagation k and polarization u are parallel to each other when longitudinal ultrasound is used.

We now turn to the thermoelectric effect, which is also unique in characterizing QPTs for its sensitivity to Fermi-surface change. It has been previously studied in the canonical heavy-fermion compound $YbRh_2Si_2$,[16] yielding strong evidence for an abrupt Fermi-surface change at the QCP. In Fig. 3, we show the isothermal thermoelectric coefficient $S(B)$ measured at various temperatures for CePdAl. A pronounced maximum arising from magnetic scattering is observed in the field window where the sequence of the metamagnetic transitions takes place. While the position of the maximum, marked by downward arrow, traces roughly the metamagnetic B_{cp} line (see Fig. 1(a)), unfortunately one cannot clearly identify any of the three metamagnetic transitions. Markedly, at high field $B > B_{\rm FL}$ (upward arrow), the value of $S(B)$ remains approximately constant, as expected from a heavy Fermi-liquid with a large Fermi-surface volume that incorporates both the local moments and the conduction electrons. Note that, there appears a valley between the broad maximum and the flat $S(B)$ at $B > B_{\rm FL}$, which falls into the extended intermediate phase space between the AFM and the heavy Fermi-liquid phase. This feature cannot be simply related to the p phase, but is most likely a signature of the thermally-broadened, small-to-large Fermi-surface crossover as indicated by the B^* line.

Though the metamagnetic transitions cannot be identified due to the low signal-to-noise ratio, the $S(B)$ curves can provide a strong evidence for the Fermi-surface change. Comparing the weakly field-dependent $S(B)$ at $B < 2$ T in the AFM phase and the nearly constant $S(B)$ at $B > B_{\rm FL}$ in the heavy Fermi-liquid phase, one immediately recognizes a change of their absolute values that is attributable to the Fermi-surface change across the Mott-type (Kondo-breakdown) line B^*. This feature becomes actually more apparent at higher temperatures simply because the absolute value of thermoelectric power increases substantially with temperature, see Fig. 3 main panel and inset. To lend further support to this inference, in Fig. 4 we compare the isothermal $S(B)$ and the Hall resistivity $\rho_{\rm H}(B)$ measured at 0.3 K (Ref. [8]). Significantly, the different $S(B)$ behaviors at low and high fields, as mentioned above, match well with the B-linear $\rho_{\rm H}(B)$ of slightly different slope in the two field intervals; see the two dashed lines on top of the $\rho_{\rm H}(B)$ data. As has been discussed previously, the large-to-small slope change of $\rho_{\rm H}(B)$ is a distinct feature of the small-to-large Fermi-surface change across the Mott-type crossover line B^* (Ref. [8]). Likewise, the afore-mentioned change of $S(B)$ between low and high field is believed to be a hallmark of the Fermi-surface change, too. The feature that the low-field $S(B)$ in the AFM phase with a small Fermi-surface is more susceptible to B in comparison to its high-field counterpart shares strong similarities with the field dependence of $\rho(B)$ (Ref. [8]), and can be ascribed to the enhanced electron scattering from spin fluctuations in the ordered phase.

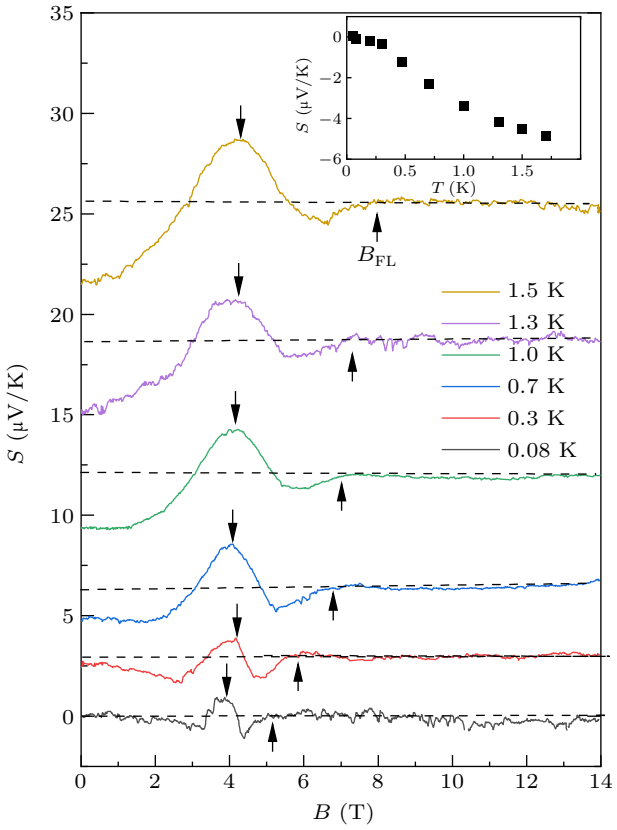


Fig. 3. Isothermal thermoelectric coefficient $S(B)$ measured at various temperatures is shown with proper offset for clarify. Inset: temperature-dependent thermoelectric coefficient $S(T)$ measured in zero field. For these measurements, the temperature gradient is applied within the *ab* plane and the magnetic field along the *c* axis. The downward arrows mark the maximums of the $S(B)$ curves, which trace roughly the metamagnetic B_{cp} line (Fig. 1(a)). The upward arrows indicate the characteristic field $B_{\rm FL}$ above which $S(B)$ tends to be constant, signalling onset of the heavy Fermi-liquid phase.

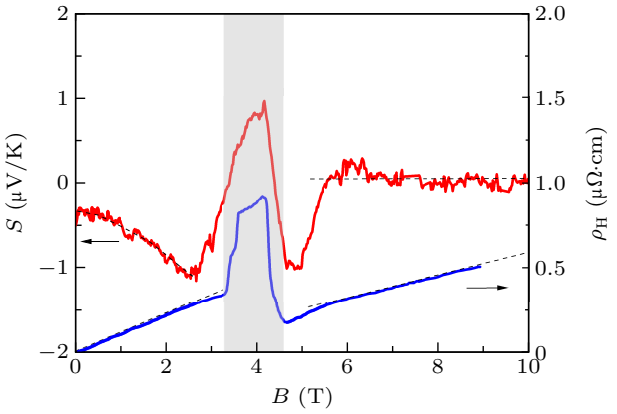


Fig. 4. The thermoelectric coefficient as a function of field is compared to the Hall resistivity[8] measured at the same temperature, $T = 0.3$ K. The shaded region indicates the field window where the sequence of metamagentic transitions and the *p* phase take place. The dashed lines on top of the $\rho_{\rm H}(B)$ data indicate the linear variation expected for Fermi liquid, and those for $S(B)$ data are guides to the eyes.

4. Conclusion

To conclude, we have shown that the metamagnetic transitions, the quantum critical phase and the Fermi-surface change across a Mott-type transition/crossover in CePdAl can be probed by ultrasonic and thermoelectric measurements at very low temperatures. In particular, the quantum critical phase can be captured by the in-plane elastic constant C_{11} rather than the out-of-plane C_{33} mode, offering a strong evidence for its existence as well as a strong implication on its origin that is most likely related to the in-plane frustration; the thermoelectric effect can probe the Fermi-surface change, complementary to the Hall-effect measurement. Though much less attention has been paid to these measurements so far, their capability to reveal distinct features on frustration-related fluctuations and Fermi-surface change promises an important role for them in characterizing complicated quantum phases.

Acknowledgments

Project supported by the National Key Research and Development Program of China (Grant No. 2017YFA0303100), the National Natural Science Foundation of China (Grant Nos. 12141002, 52088101, and 11974389), the Fund of the Chinese Academy of Sciences through the Scientific Instrument Developing Project (Grant No. ZDKYYQ20210003), the Strategic Priority Research Program (Grant No. XDB33000000), and by China Postdoctoral Science Foundation (Grant No. 2020TQ0349).

References

[1] Si Q and Steglich F 2010 *Science* **329** 1161
[2] Löhneysen H V, Rosch A, Vojta M and Wölfle P 2007 *Rev. Mod. Phys.* **79** 1015
[3] Stewart G R 2001 *Rev. Mod. Phys.* **73** 797
[4] Gegenwart P, Si Q and Steglich F 2008 *Nat. Phys.* **4** 186
[5] Doniach S 1977 *Physica B+C* **91** 231
[6] Paschen S, Lühmann T, Wirth S, Gegenwart P, Trovarelli O, Geibel C, Steglich F, Coleman P and Si Q 2004 *Nature* **432** 881
[7] Zhao H, Zhang J, Lyu M, Bachus S, Tokiwa Y, Gegenwart P, Zhang S, Cheng J G, Yang Y F, Chen G F, Isikawa Y, Si Q, Steglich F and Sun P 2019 *Nat. Phys.* **15** 1261
[8] Zhang J, Zhao H, Lv M, Hu S, Isikawa Y, Yang Y F, Si Q, Steglich F and Sun P 2018 *Phys. Rev. B* **97** 235117
[9] Dönni A, Ehlers G, Maletta H, Fischer P, Kitazawa H and Zolliker M 1996 *J. Phys.: Condens. Matter* **8** 11213
[10] Kitazawa H, Matsushita A, Matsumoto T and Suzuki T 1994 *Physica B* **199–200** 28
[11] Weber D, Yoshizawa M, Kouroudis I, Lüthi B and Walker E 1987 *Europhys. Lett.* **3** 827
[12] Thalmeier P and Lüthi B 1991 *Handbook on the Physics and Chemistry of Rare Earth*, Vol. 14, (Amsterdam: North-Holland)
[13] Lüthi B 2005 *Physical Acoustics in the Solid State* (Berlin: Springer-Verlag)
[14] Hartmann S 2010 *Thermoelectric Transport in Correlated Electron Systems*, PhD Thesis (Technical University of Dresden)
[15] Lucas S, Grube K, Huang C L, Sakai A, Wunderlich S, Green E L, Wosnitza J, Fritsch V, Gegenwart P, Stockert O and Löhneysen H V 2017 *Phys. Rev. Lett.* **118** 107204
[16] Hartmann S, Oeschler N, Krellner C, Geibel C, Paschen S and Steglich F 2010 *Phys. Rev. Lett.* **104** 096401